Journal of Visualized Experiments

Surface-enhanced resonance Raman scattering nanoprobe ratiometry for the detection of microscopic ovarian cancer via folate receptor targeting

--Manuscript Draft--

Article Type:	Methods Article - JoVE Produced Video
Manuscript Number:	JoVE58389R2
Full Title:	Surface-enhanced resonance Raman scattering nanoprobe ratiometry for the detection of microscopic ovarian cancer via folate receptor targeting
Keywords:	Raman imaging; surface enhanced Raman scattering; SERS; Nanoparticles; ovarian cancer; intraoperative; intraperitoneal; ratiometric; spectroscopy; Molecular imaging.
Corresponding Author:	Moritz Florian Kircher Memorial Sloan Kettering Cancer Center New York, NY UNITED STATES
Corresponding Author's Institution:	Memorial Sloan Kettering Cancer Center
Corresponding Author E-Mail:	kircherm@mskcc.org
Order of Authors:	Chrysafis Andreou
	Anton Oseledchyk
	Suchetan Pal
	Moritz Florian Kircher
Additional Information:	
Question	**Response**
Please indicate whether this article will be Standard Access or Open Access.	Standard Access (US$2,400)
Please indicate the **city, state/province, and country** where this article will be **filmed**. Please do not use abbreviations.	New York, NY, USA

TITLE:

Surface-Enhanced Resonance Raman Scattering Nanoprobe Ratiometry for Detecting Microscopic Ovarian Cancer *via* Folate Receptor Targeting

AUTHORS:

Chrysafis Andreou
Department of Radiology, Memorial Sloan Kettering Cancer Center, New York, NY
andreouc@mskcc.org

Anton Oseledchyk
Department of Radiology, Memorial Sloan Kettering Cancer Center, New York, NY
anton.oseledchyk@gmail.com

Suchetan Pal
Department of Radiology, Memorial Sloan Kettering Cancer Center, New York, NY
pals@mskcc.org

Moritz F. Kicher
Department of Radiology
Molecular Pharmacology Program, Sloan Kettering Institute
Center for Molecular Imaging and Nanotechnology (CMINT)
Memorial Sloan Kettering Cancer Center
Gerstner Sloan Kettering Graduate School of Biomedical Sciences
Department of Radiology, Weill Cornell Medical College of Cornell University
kircherm@mskcc.org

CORRESPONDING AUTHOR:

Moritz F. Kircher

KEYWORDS:

Raman, SERS, nanoparticle, molecular imaging, ovarian cancer, folate receptor, ratiometry.

SUMMARY:

Ovarian cancer forms metastases throughout the peritoneal cavity. Here, we present a protocol to make and use folate-receptor targeted surface-enhanced resonance Raman scattering nanoprobes that reveal these lesions with high specificity *via* ratiometric imaging. The nanoprobes are administered intraperitoneally to living mice, and the derived images correlate well with histology.

ABSTRACT:

Ovarian cancer represents the deadliest gynecologic malignancy. Most patients present at an advanced stage (FIGO stage III or IV), when local metastatic spread has already occurred. However, ovarian cancer has a unique pattern of metastatic spread, in that tumor implants are initially contained within the peritoneal cavity. This feature could enable, in principle, the

complete resection of tumor implants with curative intent. Many of these metastatic lesions are microscopic, making them hard to identify and treat. Neutralizing such micrometastases is believed to be a major goal towards eliminating tumor recurrence and achieving long-term survival. Raman imaging with surface enhanced resonance Raman scattering nanoprobes can be used to delineate microscopic tumors with high sensitivity, due to their bright and bioorthogonal spectral signatures. Here, we describe the synthesis of two 'flavors' of such nanoprobes: an antibody-functionalized one that targets the folate receptor – overexpressed in many ovarian cancers – and a non-targeted control nanoprobe with a distinct spectrum. The nanoprobes are co-administered intraperitoneally to mouse models of metastatic human ovarian adenocarcinoma. All animal studies were approved by the Institutional Animal Care and Use Committee of Memorial Sloan Kettering Cancer Center. The peritoneal cavity of the animals is surgically exposed, washed, and scanned with a Raman microphotospectrometer. Subsequently, the Raman signatures of the two nanoprobes are decoupled using a Classical Least Squares fitting algorithm, and their respective scores divided to provide a ratiometric signal of folate-targeted over untargeted probes. In this way, microscopic metastases are visualized with high specificity. The main benefit of this approach is that the local application into the peritoneal cavity – which can be done conveniently during the surgical procedure – can tag tumors without subjecting the patient to systemic nanoparticle exposure. False positive signals stemming from non-specific binding of the nanoprobes onto visceral surfaces can be eliminated by following a ratiometric approach where targeted and non-targeted nanoprobes with distinct Raman signatures are applied as a mixture. The procedure is currently still limited by the lack of a commercial wide-field Raman imaging camera system, which once available will allow for the application of this technique in the operating theater.

INTRODUCTION:

Raman imaging with 'surface enhanced Raman scattering' (SERS) nanoparticles has shown great promise in delineating lesions in a variety of settings and for many different tumor types[1-4]. The main advantage of SERS nanoparticles is their fingerprint-like spectral signature, affording them unquestionable detection that is not confounded by biological background signals[5]. Additionally, the intensity of the emitted signal is further amplified with the use of reporter molecules (dyes) with absorbance maxima in line with the excitation laser, giving rise to 'surface enhanced *resonance* Raman scattering' (SERRS) nanoparticles with even greater sensitivity[6-12].

One barrier that needs to be addressed for the adoption of SE(R)RS nanoparticles[13] and many other nanoparticle constructs[14,15] for clinical use is their mode of administration, as intravenous injection causes systemic exposure of the agent, and necessitates extensive testing to exclude potential adverse effects. In this article, we present a different paradigm based on the application of nanoparticles locally *in vivo*, directly into the peritoneal cavity during surgery, followed by a washing step to remove any unbound nanoparticles[1]. This approach is in line with novel therapeutic approaches that are currently under investigation that also make use of local instillation of agents into the peritoneal cavity, called hyperthermic intraperitoneal chemotherapy (HIPEC). Thus, the principle itself should be relatively easy to integrate into a clinical workflow. We have studied the biodistribution of the nanoparticles after intraperitoneal

application, and have not observed any detectable absorption into the systemic circulation[1]. Additionally, the local application approach circumvents the sequestration of nanoparticles by the reticuloendothelial system, so the numbers of nanoparticles required are markedly reduced. However, when applied topically, antibody-functionalized nanoparticles tend to adhere onto the visceral surfaces even in the absence of their target. In order to minimize false positive signals due to non-specific nanoparticle adhesion, we pursue a ratiometric approach, where a molecularly targeted nanoprobe provides the specific signal, and a non-targeted control nanoprobe, with different Raman spectrum, accounts for non-specific background[16,17]. We have demonstrated this methodology of topically applied surface enhanced resonance Raman ratiometric spectroscopy recently in a mouse model of diffuse ovarian cancer[1].

The overall goal of this method is to develop two SERRS nanoprobes, one targeted and one non-specific, to be applied locally in mouse models, in order to image the prevalence/overexpression of a cancer related biomarker using ratiometric detection of the two probes *via* Raman imaging. In this work, the folate receptor (FR) was chosen as the target, as this is a marker upregulated in many ovarian cancers[18,19]. Raman microimaging with SERS-based nanoparticles has also been demonstrated for cancer cell identification[20]. Two distinct "flavors" of Raman nanoparticles are synthesized, each deriving its fingerprint from a different organic dye. The nanoparticles consist of a star-shaped gold core surrounded by a silica shell and demonstrate surface plasmon resonance at approximately 710 nm. The Raman reporter (organic dye) is deposited concurrently with the formation of silica shell. Finally, for the FR-targeted nanoprobes (αFR-NPs) the silica shell is conjugated with antibodies, whereas the non-targeted nanoprobes (nt-NPs) are passivated with a monolayer of polyethylene glycol (PEG).

This technique was successfully used to map microscopic tumors in a mouse xenograft model of diffuse metastatic ovarian cancer (SKOV-3), demonstrating its applicability for *in vivo* use. It can also be extended for use in excised tissues, for tumor phenotyping, or margin determination after debulking as shown in a cognate study[21].

SERRS nanoprobes provide a robust platform for the creation of multiple targeted tags for biomarkers, synthesized with straightforward chemical reactions as outlined schematically in **Figure 1**. Here, we present the protocol for the synthesis of the two types of SERRS nanoprobes (sections 1-3), the development of a suitable ovarian cancer mouse model (section 4), the administration of nanoprobes and imaging (section 5), and finally the data analysis and visualization (section 6).

PROCEDURE:

All animal studies were approved by the Institutional Animal Care and Use Committee of Memorial Sloan Kettering Cancer Center (#06-07-011).

1) Gold Nanostar Core Synthesis

Note: Gold nanostars are used as cores for both flavors of SERRS nanoprobes used in this experiment.

1.1) Prepare 800 mL of 60 mM ascorbic acid ($C_6H_8O_6$) solution in deionized (DI) water and 8 mL of 20 mM tetrachloroauric acid ($HAuCl_4$) solution in DI water. Cool to 4 °C.

1.2) Perform this reaction step at 4 °C. Place a conical flask containing 800 mL of the ascorbic acid solution on a magnetic stir plate and induce a steady vortex. Quickly add 8 mL of the tetrachloroauric acid solution into the vortex. Within seconds, nanostars will form and the solution will assume a dark blue color. In case the color at any time becomes pink or purple, signifying the formation of nanospheres, the suspension should be discarded and the synthesis reattempted.

1.3) Pour the nanostar suspension into 50 mL conical tubes, and centrifuge for 20 min (4 °C, 3,320 × g). Aspirate the supernatant leaving approximate 200 µL of the solution in each tube. Pay caution not to disturb the pellet of nanoparticles at the bottom of the tube.

Note: The supernatant should have a blue tint because of remaining suspended nanostars.

1.4) Using a micropipette, agitate the solution to suspend and collect the nanoparticles from each tube. Part of the pellet may be compacted on the bottom of the tube and will not resuspend even with vigorous pipetting—discard this part.

1.5) Transfer the nanoparticle suspension to a dialysis cassette (MWCO 3.5 kDa) and dialyze at least three days against 2 L of DI water, changing the water daily. Store nanostars in dialysis at 4 °C for up to a month with water changes every 3-4 days.

Note: The nanostars should be kept in dialysis until required for the silication reaction, as described in section 2.

2) Formation of the Silica Shell

NOTE: Two flavors of Raman nanoprobes are synthesized. The synthesis procedure is the same for both, with the only difference being the Raman reporter molecule (dye) used. In this experiment, IR780 perchlorate and IR140 are used. The reaction should always be performed in **plastic** containers. The synthesis is highly scalable and can be adjusted for the desired amount of injectate required. Here, a medium batch synthesis is described, which can be scaled linearly to lower or higher volumes as needed, with the same concentrations and reaction times. The reactions for the two SERRS nanoprobe types can be performed in parallel. Pay attention to avoid cross-contamination. Sonication should be performed for the redispersion of nanoparticle pellets after centrifugation during washing steps, or after the nanoparticles were stored for longer than one hour. Sonication should be performed until the nanoparticles are clearly suspended into the solution, typically for 1 s.

2.1) In Tube A (a 50 mL conical tube), mix 10 mL of isopropanol, 500 µL of TEOS, 200 µL of DI water, and 60 µL of dye (IR780 perchlorate or IR140, 20 mM in DMF (dimethylformamide)).

2.2) In Tube B (15 mL conical tube), mix 3 mL of ethanol and 200 µL of ammonium hydroxide. Sonicate the nanostars from Step 1.4 to disperse any clusters in solution and add 1.2 mL of nanostars to the tube.

Note: the ammonium hydroxide solution is highly volatile and hard to pipette accurately. Store it at 4 °C, until needed, to facilitate pipetting.

2.3) Place Tube A on a vortex mixer and induce a steady vortex. Rapidly add the contents of Tube B into the vortex and keep mixing for about 5 s. Immediately transfer to a shaker and let react for 15 min while shaking at 300 rpm, at room temperature.

2.4) After the 15 min incubation, quench the reaction by adding ethanol to fill the 50 mL tube. Centrifuge for 20 min at 3,220 × g and 4 °C.

2.5) Aspirate the supernatant, leaving about 0.5 mL of solution, being careful not to disturb the pellet. Add 1 mL of ethanol and agitate with a pipette to resuspend the nanoparticles. Transfer to a 1.5 mL centrifuge tube and wash 4 times with ethanol by centrifuging at 11,000 × g for 4 min, aspirating the supernatant, and resuspending the pellet by ultrasonication for approximately 1 s.

Note: At this stage, the silicated nanoparticles can be functionalized, as described in section 3, or resuspended in DI water with an extra washing step, for storage at 4 °C for up to a week.

3) Surface Functionalization

Note: IR780 SERRS nanoprobes will be conjugated with folate receptor-targeting antibodies *via* a PEG crosslinker to form αFR-NPs; IR140 SERRS control nanoprobes will be conjugated with a passivating PEG monolayer, for nt-NPs. Both flavors are formed *via* a thiol-maleimide reaction in separate but parallel reactions.

3.1) Wash nanoparticles twice by centrifuging at 11,000 × g for 4 min, aspirating the supernatant, and resuspending the pellet in 1 mL of ethanol by ultrasonication. Repeat the washing step once more, but redisperse in 1 mL of 85% ethanol, 10% 3-MPTMS (3-mercaptopropyltrimethoxysilane), and 5% DI water. Incubate at room temperature for 1–2 h to introduce thiols on the particle surface.

3.2) Wash the thiol-functionalized nanoparticles by centrifuging at 11,000 × g for 4 min, aspirating the supernatant and resuspending the pellet by ultrasonication, twice in ethanol, twice in DI, and finally in HEPES (4-(2-hydroxyethyl)-1-piperazineethanesulfonic acid) buffer (10 mM, pH 7.1), and set aside.

Note: MES (2-(*N*-morpholino)ethanesulfonic acid) buffer or HEPES should be used. Buffers with higher salinity, such as PBS (phosphate-buffered saline), may induce nanoparticle aggregation.

3.3) For the antibody functionalized αFR-NPs, react 200 µg of antibodies (anti-folate binding protein antibody clone [LK26]) with tenfold molar excess of PEG crosslinker (poly(ethylene glycol)(N-hydroxysuccinimide 5-pentanoate) ether N'-(3-maleimidopropionyl) aminoethane (CAS: 851040-94-3), in dimethyl sulfoxide (DMSO)) in 500 µL of MES buffer (10 mM, pH 7.1) for 30 min.

3.4) Remove excess crosslinker and concentrate antibody by centrifuging the antibody-PEG solution in a centrifugal filter (MWCO 100 kDa). For the centrifugal filters used in this study, perform centrifugation for 10 min at 14,000 × g and 23 °C. Recover the conjugated antibodies in a fresh tube by inverting the filter and centrifuging at 1,000 × g for 2 min.

3.5) Pipette the IR780 nanoparticles from Step 3.2 into the tube with the antibodies and agitate with the pipette to mix. Incubate the mixture for at least 30 min at room temperature, or, alternatively at 4 °C overnight to form the αFR-NPs.

3.6) To form nt-NPs, add 1% w/v methoxy-terminated (m)PEG5000-maleimide (CAS: 99126-64-4) dissolved in DMSO to the IR140 SERRS nanoparticles from Step 3.2 and let react in 500 µL MES buffer (10 mM, pH 7.1) for at least 30 min at room temperature, or, alternatively at 4 °C overnight.

3.7) For administration to mice (Section 5), spin down both nanoprobe flavors at 11,000 × g for 4 min, aspirate the supernatant to remove solution with free unreacted antibodies/PEG, and redisperse each flavor in MES buffer (10 mM, pH 7.1) at 600 pM concentration. When resuspending the nanoparticles, minimize unnecessary exposure to the ultrasound, to prevent denaturation of the antibody.

4) Mouse Model Development

4.1) Establish a steady culture of human ovarian adenocarcinoma (SKOV-3) cell line. Optionally, to enable monitoring *via* bioluminescence/fluorescence, use transfected SKOV-3 $^{Luc+/GFP+}$ cells. Culture cells in RPMI (Roswell Park Memorial Institute) medium with 10% fetal calf serum and passage twice a week. For injection, incubate cells with 0.25% trypsin/0.05% EDTA for 3 min to detach, and subsequently wash and resuspend in PBS at 2×10^6 cells/100 µL.

4.2) To establish the ovarian micrometastasis model, inject 200 µL of suspended SKOV-3 cells intraperitoneally into athymic female mice (FOXn1nu/FOXn1nu mice, 6-8 weeks old). Disseminated peritoneal spread will occur in approximately 4 weeks. If using SKOV-3 $^{Luc+}$ cells, tumor growth can be monitored with bioluminescence by administering 2 mg of beetle luciferin in 50 µL PBS *via* retroorbital injection.

5) Nanoprobe Injection and Imaging

5.1) Prepare nanoprobes (αFR-NPs and nt-NPs) as described in Sections 1–3 and mix at a 1:1 ratio, for a final concentration of 300 pM of each type in MES buffer (10 mM, pH 7.1). Optionally, prepare reference standards of 30 pM of each of the nanoprobe flavors in small (100 µL) conical tubes.

5.2) Inject intraperitoneally 1 mL of the nanoparticle suspension in each mouse and gently massage the belly to distribute the nanoparticles within the peritoneal cavity. Return the mouse to its housing. After 25 or more minutes, euthanize the mouse *via* CO_2 asphyxiation.

5.3) Fasten the mouse on a surgical platform, at the supine position (for whole abdomen imaging, the platform needs to be mountable onto the upright microscope stage).

5.3.1. Using serrated forceps and dissection scissors, remove the skin to expose the peritoneum and perform a large sagittal incision (between 2 and 3 cm in length) to expose the whole abdomen. Attach the peritoneal flaps onto the platform. Wash the inside of the peritoneal cavity with at least 60 mL of PBS using a plastic squirt bottle.

Note: To enable unobstructed imaging of the whole abdomen, the intestines need to be mobilized or excised. For excision, resect with a ligation of the mesenteric vessels in order to reduce hemorrhage into the abdominal cavity.

5.3.2. Alternatively, to image specific organs, excise them after the PBS wash, and place them onto a microscope slide.

5.4) Transfer the platform or slide to a Raman microspectrophotometer with upright optical configuration and a motorized stage for imaging; use a commercial system with a 300 mW 785 nm diode laser, with a grating of 1200 grooves per mm, centered at 1115 cm^{-1}.

5.4.1. Focus on the area of interest using white light optics, parfocal with the Raman laser. Select the area to be imaged and the desired resolution; in this report a high-speed acquisition mode was used (spectra acquired under continuous laser illumination with the microscope stage constantly moving, with effective spatial resolution 14.2 µm by 200 µm; at 5X magnification, 100 mW power at objective, and <100 ms exposure per point).

Note: The tubes with the reference nanoprobes from step 5.1 can be placed within the imaged area if desired, to provide internal reference standards for the subsequent analysis. Make sure no extraneous light sources other than the laser reach the objective.

5.5) Optionally, prepare the sample for histological processing and validation by fixation in 4% paraformaldehyde in PBS overnight at 4 °C. Rinse with PBS at 4 °C for 15 min at least twice. Keep the sample in 70% ethanol in water until standard histological processing and paraffin embedding. For histological validation of the tumors, sections (5 µm thick) from different depths of the paraffin block can be stained with hematoxylin and eosin (H&E).

6) Data Processing and Visualization

Note: All data processing was performed with a graphical user interface developed in-house, using commercial software. All of the functions used have generic equivalents available in other computing environments.

6.1) Obtain reference spectra for the two flavors, by interrogating pure suspensions of each. The reference spectra can be derived from point scans of the nanoprobes, imaging of the nanoprobes in well-plates, or by including internal references in the experimental scans in the reference tubes (see Step 5.1).

6.2) Preprocess the reference spectra, by using baseline subtraction (Whittaker filter, λ=200), normalization by the area under the curve, and Savitzky-Golay derivative filter (second-degree polynomial fit, first-order derivative, width = 15 steps). These preprocessed spectra will serve as references for the classical least squares (CLS) model.

6.3) Preprocess the sample data from the image in the same way as the reference spectra. Obtain CLS scores for each sample point by using an available CLS algorithm. The direct CLS (DCLS) scores are simply the coordinates of the projection of a sample spectrum onto the linear space defined by the generalized inverse matrix (Moore-Penrose inverse) of the reference spectra. Other fitting algorithms can be used (non-negative least squares, partial least squares, or others).

Note: Some fitting algorithms can give rise to negative scores, which in this context are not physical. If this is the case, a threshold could be set to exclude negative scores, or a constrained non-negative least squares algorithm be employed instead.

6.4) Calculate the pointwise ratio of the scores on the reference for the targeted nanoparticles ($Scores_{\alpha FR}$) over the scores on the reference for the non-targeted nanoparticles ($Scores_{nt}$). If the scores are non-negative, the ratio can be expressed in a logarithmic fashion:

$$R = \log_{10}(Scores_{\alpha FR} / Scores_{nt}).$$

The ratio R is best displayed in a diverging color scale centered at zero, to express the relative abundance of the probes in orders of magnitude. The resulting image can be overlaid onto the white light image of the sample, to reveal areas of folate receptor overexpression.

REPRESENTATIVE RESULTS:

For quality control purposes, the nanoparticles can be characterized using a variety of methods during the synthesis process, including TEM, DLS, nanoparticle tracking analysis, and UV/Vis absorbance spectroscopy, as shown in **Figure 2**.

In this way, the size of the gold nanostar core (described in Section 1), the formation of the silica shell (Section 2) and subsequent surface functionalization (Section 3) can be verified (**Figure 2**). Typically, the size (hydrodynamic diameter) of the gold nanostar core is expected to

be around 80 nm, and the silica shell is around 20 nm thick, making the total silicated nanoparticle size around 120 nm and around 140 nm after conjugation with the αFR-antibody. UV/Vis absorbance can also be used to verify the morphology of the nanoparticles. Nanostar cores in water typically have an absorbance maximum at 670 nm, whereas after silication the maximum shifts to around 710 nm. Absorbance maxima at lower wavelengths are a sign of either spherical morphology or aggregation. Typical reaction yields and concentrations are shown in **Table 1** and depend strongly on pipetting technique during the wash steps.

Each point obtained from the Raman scan contains a spectrum for an interrogated location. These spectra are a linear superposition of the nanoprobes' SERRS signal and any background fluorescence. The spectra can be processed to remove the fluorescence and normalized to unit area to compensate for signal strength, prior to applying the CLS model (described in section 6), as shown in **Figure 3**. Representative images for scores on each of the nanoprobe reference spectra and their pointwise ratio are shown in **Figure 4**. Although each score individually does not provide specific localization of tumors, the ratio reveals the presence of disseminated microscopic spread.

Tables and Figures

Table 1. Nanoparticle yield after each reaction step. The concentrations are approximate. The yield was determined by nanoparticle tracking analysis, with two independent syntheses and 5 independent measurements from each.

Figure 1: Schematic of synthesis and application of ratiometric SERRS nanoprobe imaging. **(**1) Gold nanostars are synthesized as described in section 1. (2) A silica shell is formed around the gold nanostar cores and Raman reporter molecules (infrared dyes IR-780 perchlorate and IR-140) are used to create two distinct nanoparticle flavors, as described in section 2. (3) The surface of the nanoparticles is coated with thiols, as described in section 3.1, to enable further surface functionalization. The IR-780 flavor nanoparticles are conjugated with an anti-Folate Receptor antibody, while the IR-140 ones are passivated with a layer of PEG-5k as described in sections 3.3 to 3.6. (4) A mouse model of diffuse intraperitoneal ovarian metastatic spread is developed as described in section 4, and when ready, the SERRS nanoprobes are administered intraperitoneally. (5) The mice are euthanized, and the abdomen surgically exposed to enable Raman imaging as described in section 5. (6) The Raman spectra are analyzed pointwise to determine the relative abundance of the two probes and generate a ratiometric map of folate receptor overexpression as described in section 6.

Figure 2: Physical characterization of SERRS nanoprobes. The nanoparticles can be subjected to quality control after each part of the synthesis. Transmission electron microscopy (TEM) reveals the shape of the gold core and the successful formation of the silica shell without nanoparticle aggregation; scale bar is 100 nm. Dynamic light scattering (DLS) can measure the size and ζ-potential of the nanoparticles to verify successful silication and functionalization. UV/Vis absorbance can be used to confirm the presence of a plasmonic peak around 670 nm for the nanostars, shifting to 710 nm after silication. Raman measurements reveal the presence of

the unique spectra of each flavor throughout the synthesis. The intensity of the nanostar spectrum, with no characteristic peaks, was amplified by 100× for emphasis.

Figure 3: Processing of Raman spectra. Raw spectra consist of the nanoprobes' SERRS signature, superimposed on top of a wide fluorescence band. With baseline subtraction the fluorescence band is removed, and the Raman peaks become prominent. In order to detect the spectral signature of the nanoparticles irrespective of intensity, each spectrum (references and samples alike) is normalized to unit area. Finally, a smoothing-derivative filter is applied to boost the Raman peaks, while reducing noise. The processed reference spectra are used to develop a CLS model, in order to classify the processed sample spectra based on the ratio R.

Figure 4: Ratiometric imaging of ovarian cancer micrometastases in the abdomen. Raman imaging of the exposed abdomen of a mouse, featuring extensive ovarian metastases as revealed by bioluminescence imaging. Each point of the scan features a spectrum, which is processed (section 6, **Figure** 3) and scored based on a CLS model, to obtain scores on the two references: αFR-NP shown in red, and nt-NP in blue. The scores are then divided pointwise, to reveal the relative abundance of the two probes as a ratio. Optionally, by thresholding the ratio, the "positive" areas can be superimposed onto an optical image of the abdomen, to allow resection or other focused treatments. Figure is an adapted version from Ref. 1, with permission from the journal.

DISCUSSION:

The protocol described here provides instruction for the synthesis of two "flavors" of SERRS nanoprobes, and their employment in mice for Raman imaging of ovarian tumor overexpressing the Folate Receptor, using a ratiometric algorithm. The main advantage of Raman imaging over other optical imaging techniques (such as fluorescence) is the high specificity of the nanoprobe signal that cannot be confounded with any signals of biological origin. In this embodiment of Raman imaging, the nanoparticles are not administered intravenously, but locally, *via* an intraperitoneal injection followed by a single washing step. This methodology, once translated into the clinical arena, would represent an elegant solution to enable surgeons to visualize and therefore resect all ovarian cancer implants, even those that are too small to detect with the naked eye, and which cannot be targeted with a systemically injected imaging agent due to their lack of feeding vessels connected to the systemic circulation. At the same time, as our SERRS nanoparticles are not resorbed into the systemic circulation, potential concerns for side effects are minimized. Our study is one example of the growing evidence that carefully designed nanoconstructs can provide unique advantages over conventional imaging and therapy technologies[22-38].

The SERRS nanoprobes described here are biologically inert and have been employed for tumor delineation in mouse models of several cancer types. The reaction for the formation of the silica shell (concurrent with reporter dye encapsulation) is an improved version of our previously reported synthesis[1,7,8], which is less prone to nanoparticle aggregation and the formation of "free silica" nanoparticles (without gold core). The reaction can be used with a variety of commercially available infrared organic dyes, in addition to the ones presented here, to yield a

large collection of Raman flavors. The resulting signal intensity, however, depends on the dye's affinity to gold, and other factors. Additionally, the amount of dye added to the reaction should be determined on a per-dye basis, as certain molecules and their counterions cause aggregation of the gold nanostars more than others. In the case of severe nanoparticle aggregation, the amount of dye used should be decreased. Aggregation of the gold cores is undesirable, as it can cause severe variability in the Raman signal intensity and complicate the acquired data. The formation of free silica is for the most part innocuous, as it provides no Raman signal. However, during functionalization the antibodies will adhere to silica nanoparticles, diminishing the overall targeting effectiveness of the method. The thickness of the silica shell depends on reaction time, temperature, and the amount of water added (Step 2.1). If the resulting silica shell is deemed too thin (**Figure 1**, top right), one or more of these parameters can be increased appropriately.

With regards to data acquisition, its quality greatly depends on the brightness of the nanoprobes. This becomes particularly apparent when performing rapid Raman acquisition, as described in Section 5. To make sure that the data is sufficiently discernible from the noise, the spectra should be inspected, and the presence of the representative Raman peaks of the probes verified. If the signal is too weak, the exposure time per point can be increased. However, this approach can lead to prohibitively long scans or very low spatial resolution. To ensure reproducibility and consistency, calibration of the Raman scanner should be performed according to the manufacturer's recommendation and is typically done using a common standard (*e.g.,* a silicon wafer).

One of the main strengths of this method is its versatility. Different tumor types can be imaged by using specific antibodies targeting different molecular markers. Additionally, the nanoprobes described here can be administered to animal models – intraperitoneally or intravenously – but also, using the same techniques, they can be used to stain tissues, either fixed or freshly excised.

Although the ratiometric technique provides specificity for detection of microscopic tumors, the distribution of the individual probes is not specific to the tumor areas. This means that theranostic techniques such as photothermal/photodynamic therapy or drug-loading would not be ideal, as the therapy would be delivered to healthy areas as well. One potential therapeutic application afforded by this technique would be the automated ablation of microtumors after ratiometric detection.

We hope that this local, ratiometric approach of Raman imaging can pave the way for using SERRS nanoprobes, after the necessary clinical trials, as a molecular imaging agent in patients. This method was developed to be compatible with potential future applications in humans, as the nanoparticles could be administered to and removed from the abdominal cavity using devices that are already in clinical use for HIPEC.

ACKNOWLEDGMENTS:

The following funding sources (to M.F.K.) are acknowledged: NIH R01 EB017748, R01 CA222836 and K08 CA16396; Damon Runyon-Rachleff Innovation Award DRR-29-14, Pershing Square Sohn Prize by the Pershing Square Sohn Cancer Research Alliance, and MSKCC Center for Molecular Imaging & Nanotechnology (CMINT) and Technology Development Grants. Acknowledgments are also extended to the grant-funding support provided by the MSKCC NIH Core Grant (P30-CA008748).

DISCLOSURES

- M.F.K. is listed as an inventor on several issued or pending patent applications related to this work. M.F.K. is a co-founder of RIO Imaging, Inc., which aims at translating SERRS nanoparticles into the clinics.
- The authors declare that they have no other competing financial interests.

REFERENCES

1 Oseledchyk, A., Andreou, C., Wall, M. A. & Kircher, M. F. Folate-Targeted Surface-Enhanced Resonance Raman Scattering Nanoprobe Ratiometry for Detection of Microscopic Ovarian Cancer. *ACS Nano.* **11** (2), 1488-1497, doi:10.1021/acsnano.6b06796, (2017).

2 Andreou, C. *et al.* Imaging of Liver Tumors Using Surface-Enhanced Raman Scattering Nanoparticles. *ACS Nano.* **10** (5), 5015-5026, doi:10.1021/acsnano.5b07200, (2016).

3 Karabeber, H. *et al.* Guiding brain tumor resection using surface-enhanced Raman scattering nanoparticles and a hand-held Raman scanner. *ACS Nano.* **8** (10), 9755-9766, doi:10.1021/nn503948b, (2014).

4 Kircher, M. F. *et al.* A brain tumor molecular imaging strategy using a new triple-modality MRI-photoacoustic-Raman nanoparticle. *Nature Medicine.* **18** (5), 829-834, doi:10.1038/nm.2721, (2012).

5 Andreou, C., Kishore, S. A. & Kircher, M. F. Surface-Enhanced Raman Spectroscopy: A New Modality for Cancer Imaging. *Journal of Nuclear Medicine.* **56** (9), 1295-1299, doi:10.2967/jnumed.115.158196, (2015).

6 Harmsen, S. *et al.* Rational design of a chalcogenopyrylium-based surface-enhanced resonance Raman scattering nanoprobe with attomolar sensitivity. *Nature Communications.* **6** 6570, doi:10.1038/ncomms7570, (2015).

7 Harmsen, S. *et al.* Surface-enhanced resonance Raman scattering nanostars for high-precision cancer imaging. *Science Translational Medicine.* **7** (271), 271ra277, doi:10.1126/scitranslmed.3010633, (2015).

8 Harmsen, S., Wall, M. A., Huang, R. & Kircher, M. F. Cancer imaging using surface-enhanced resonance Raman scattering nanoparticles. *Nature Protocols.* **12** (7), 1400-1414, doi:10.1038/nprot.2017.031, (2017).

9 Huang, R. *et al.* High Precision Imaging of Microscopic Spread of Glioblastoma with a Targeted Ultrasensitive SERRS Molecular Imaging Probe. *Theranostics.* **6** (8), 1075-1084, doi:10.7150/thno.13842, (2016).

10 Iacono, P., Karabeber, H. & Kircher, M. F. A "schizophotonic" all-in-one nanoparticle coating for multiplexed SE(R)RS biomedical imaging. *Angewandte Chemie, International Edition in English.* **53** (44), 11756-11761, doi:10.1002/anie.201403835, (2014).

11 Spaliviero, M. *et al.* Detection of Lymph Node Metastases with SERRS Nanoparticles. *Molecular Imaging and Biology.* **18** (5), 677-685, doi:10.1007/s11307-016-0932-2, (2016).
12 Nayak, T. R. *et al.* Tissue factor-specific ultra-bright SERRS nanostars for Raman detection of pulmonary micrometastases. *Nanoscale.* **9** (3), 1110-1119, doi:10.1039/c6nr08217c, (2017).
13 Thakor, A. S. *et al.* The fate and toxicity of Raman-active silica-gold nanoparticles in mice. *Science Translational Medicine.* **3** (79), 79ra33, doi:10.1126/scitranslmed.3001963, (2011).
14 Liu, J. *et al.* Effects of Cd-based Quantum Dot Exposure on the Reproduction and Offspring of Kunming Mice over Multiple Generations. *Nanotheranostics.* **1** (1), 23-37, doi:10.7150/ntno.17753, (2017).
15 Wu, N. *et al.* The biocompatibility studies of polymer dots on pregnant mice and fetuses. *Nanotheranostics.* **1** (3), 261-271, doi:10.7150/ntno.18964, (2017).
16 Garai, E. *et al.* High-sensitivity, real-time, ratiometric imaging of surface-enhanced Raman scattering nanoparticles with a clinically translatable Raman endoscope device. *Journal of Biomedical Optics.* **18** (9), 096008, doi:10.1117/1.JBO.18.9.096008, (2013).
17 Wang, Y. W. *et al.* Rapid ratiometric biomarker detection with topically applied SERS nanoparticles. *Technology (Singap World Sci).* **2** (2), 118-132, doi:10.1142/S2339547814500125, (2014).
18 Lengyel, E. Ovarian cancer development and metastasis. *American Journal of Pathology.* **177** (3), 1053-1064, doi:10.2353/ajpath.2010.100105, (2010).
19 Vergote, I. B., Marth, C. & Coleman, R. L. Role of the folate receptor in ovarian cancer treatment: evidence, mechanism, and clinical implications. *Cancer and Metastasis Reviews.* **34** (1), 41-52, doi:10.1007/s10555-014-9539-8, (2015).
20 Fasolato, C. *et al.* Folate-based single cell screening using surface enhanced Raman microimaging. *Nanoscale.* **8** (39), 17304-17313, doi:10.1039/c6nr05057c, (2016).
21 Wang, Y. W. *et al.* Raman-Encoded Molecular Imaging with Topically Applied SERS Nanoparticles for Intraoperative Guidance of Lumpectomy. *Cancer Research.* **77** (16), 4506-4516, doi:10.1158/0008-5472.CAN-17-0709, (2017).
22 Andreou, C., Pal, S., Rotter, L., Yang, J. & Kircher, M. F. Molecular Imaging in Nanotechnology and Theranostics. *Molecular Imaging and Biology.* **19** (3), 363-372, doi:10.1007/s11307-017-1056-z, (2017).
23 Chitgupi, U., Qin, Y. & Lovell, J. F. Targeted Nanomaterials for Phototherapy. *Nanotheranostics.* **1** (1), 38-58, doi:10.7150/ntno.17694, (2017).
24 Choi, D. *et al.* Iodinated Echogenic Glycol Chitosan Nanoparticles for X-ray CT/US Dual Imaging of Tumor. *Nanotheranostics.* **2** (2), 117-127, doi:10.7150/ntno.18643, (2018).
25 Dubey, R. D. *et al.* Novel Hyaluronic Acid Conjugates for Dual Nuclear Imaging and Therapy in CD44-Expressing Tumors in Mice In Vivo. *Nanotheranostics.* **1** (1), 59-79, doi:10.7150/ntno.17896, (2017).
26 Gupta, M. K. *et al.* Recent strategies to design vascular theranostic nanoparticles. *Nanotheranostics.* **1** (2), 166-177, doi:10.7150/ntno.18531, (2017).
27 Huang, Y. J. & Hsu, S. H. TRAIL-functionalized gold nanoparticles selectively trigger apoptosis in polarized macrophages. *Nanotheranostics.* **1** (3), 326-337, doi:10.7150/ntno.20233, (2017).

28 Pal, S., Harmsen, S., Oseledchyk, A., Hsu, H. T. & Kircher, M. F. MUC1 Aptamer Targeted SERS Nanoprobes. *Advanced Functional Materials.* **27** (32), doi:10.1002/adfm.201606632, (2017).
29 Zanganeh, S. *et al.* Iron oxide nanoparticles inhibit tumour growth by inducing pro-inflammatory macrophage polarization in tumour tissues. *Nat Nanotechnol.* **11** (11), 986-994, doi:10.1038/nnano.2016.168, (2016).
30 Lee, J., Lee, Y. M., Kim, J. & Kim, W. J. Doxorubicin/Ce6-Loaded Nanoparticle Coated with Polymer *via* Singlet Oxygen-Sensitive Linker for Photodynamically Assisted Chemotherapy. *Nanotheranostics.* **1** (2), 196-207, doi:10.7150/ntno.18576, (2017).
31 Li, R., Zheng, K., Yuan, C., Chen, Z. & Huang, M. Be Active or Not: the Relative Contribution of Active and Passive Tumor Targeting of Nanomaterials. *Nanotheranostics.* **1** (4), 346-357, doi:10.7150/ntno.19380, (2017).
32 Lin, S. Y., Huang, R. Y., Liao, W. C., Chuang, C. C. & Chang, C. W. Multifunctional PEGylated Albumin/IR780/Iron Oxide Nanocomplexes for Cancer Photothermal Therapy and MR Imaging. *Nanotheranostics.* **2** (2), 106-116, doi:10.7150/ntno.19379, (2018).
33 Roberts, S. *et al.* Sonophore-enhanced nanoemulsions for optoacoustic imaging of cancer. *Chemical Science (Royal Society of Chemistry: 2010).* **9** (25), 5646-5657, doi:10.1039/c8sc01706a, (2018).
34 Liu, L., Ruan, Z., Yuan, P., Li, T. & Yan, L. Oxygen Self-Sufficient Amphiphilic Polypeptide Nanoparticles Encapsulating BODIPY for Potential Near Infrared Imaging-guided Photodynamic Therapy at Low Energy. *Nanotheranostics.* **2** (1), 59-69, doi:10.7150/ntno.22754, (2018).
35 Liu, R., Tang, J., Xu, Y., Zhou, Y. & Dai, Z. Nano-sized Indocyanine Green J-aggregate as a One-component Theranostic Agent. *Nanotheranostics.* **1** (4), 430-439, doi:10.7150/ntno.19935, (2017).
36 Sneider, A., VanDyke, D., Paliwal, S. & Rai, P. Remotely Triggered Nano-Theranostics For Cancer Applications. *Nanotheranostics.* **1** (1), 1-22, doi:10.7150/ntno.17109, (2017).
37 Wall, M. A. *et al.* Surfactant-Free Shape Control of Gold Nanoparticles Enabled by Unified Theoretical Framework of Nanocrystal Synthesis. *Advanced Materials.* **29** (21), doi:10.1002/adma.201605622, (2017).
38 Sonali *et al.* Nanotheranostics: Emerging Strategies for Early Diagnosis and Therapy of Brain Cancer. *Nanotheranostics.* **2** (1), 70-86, doi:10.7150/ntno.21638, (2018).

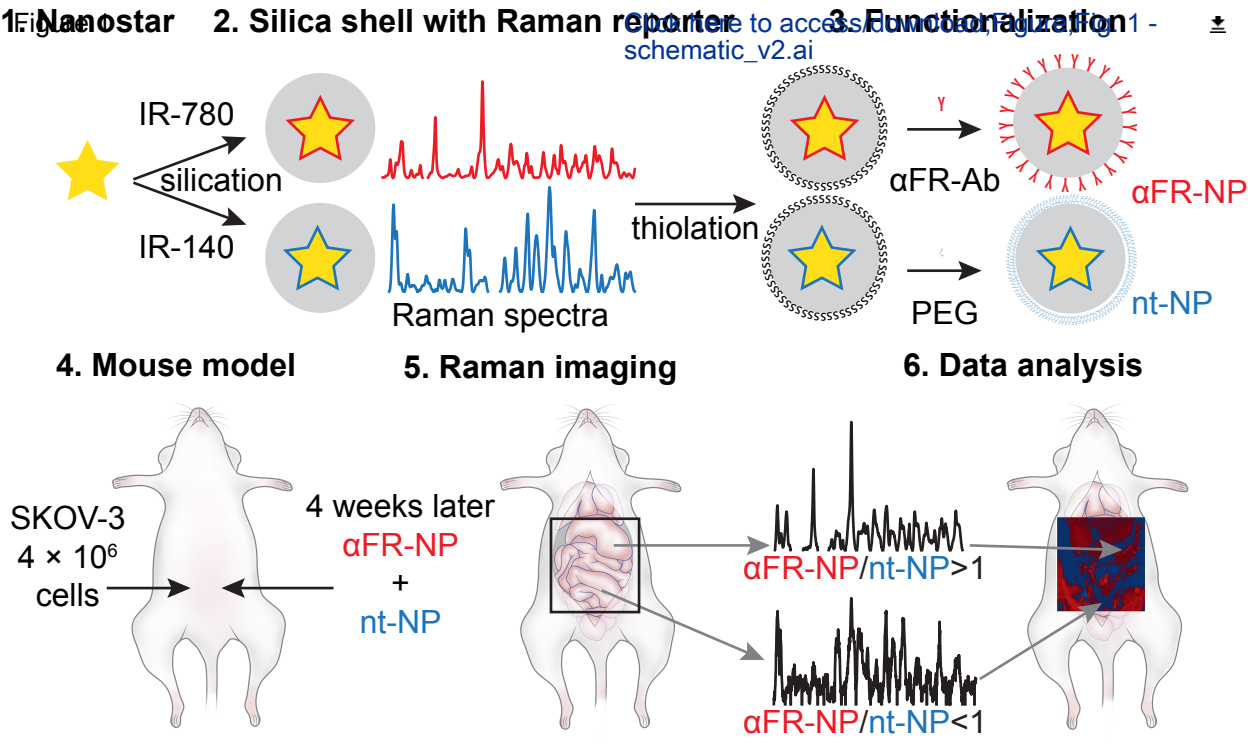
1. Nanostar
2. Silica shell with Raman reporter
3. Functionalization
Figure 1
Subscribe to access Annotated Figure 1 - schematic_v2.ai
IR-780
silication
IR-140
Raman spectra
thiolation
αFR-Ab
αFR-NP
PEG
nt-NP
4. Mouse model
5. Raman imaging
6. Data analysis
SKOV-3
4 × 10^6
cells
4 weeks later
αFR-NP
+
nt-NP
αFR-NP/nt-NP>1
αFR-NP/nt-NP<1

Figure 2

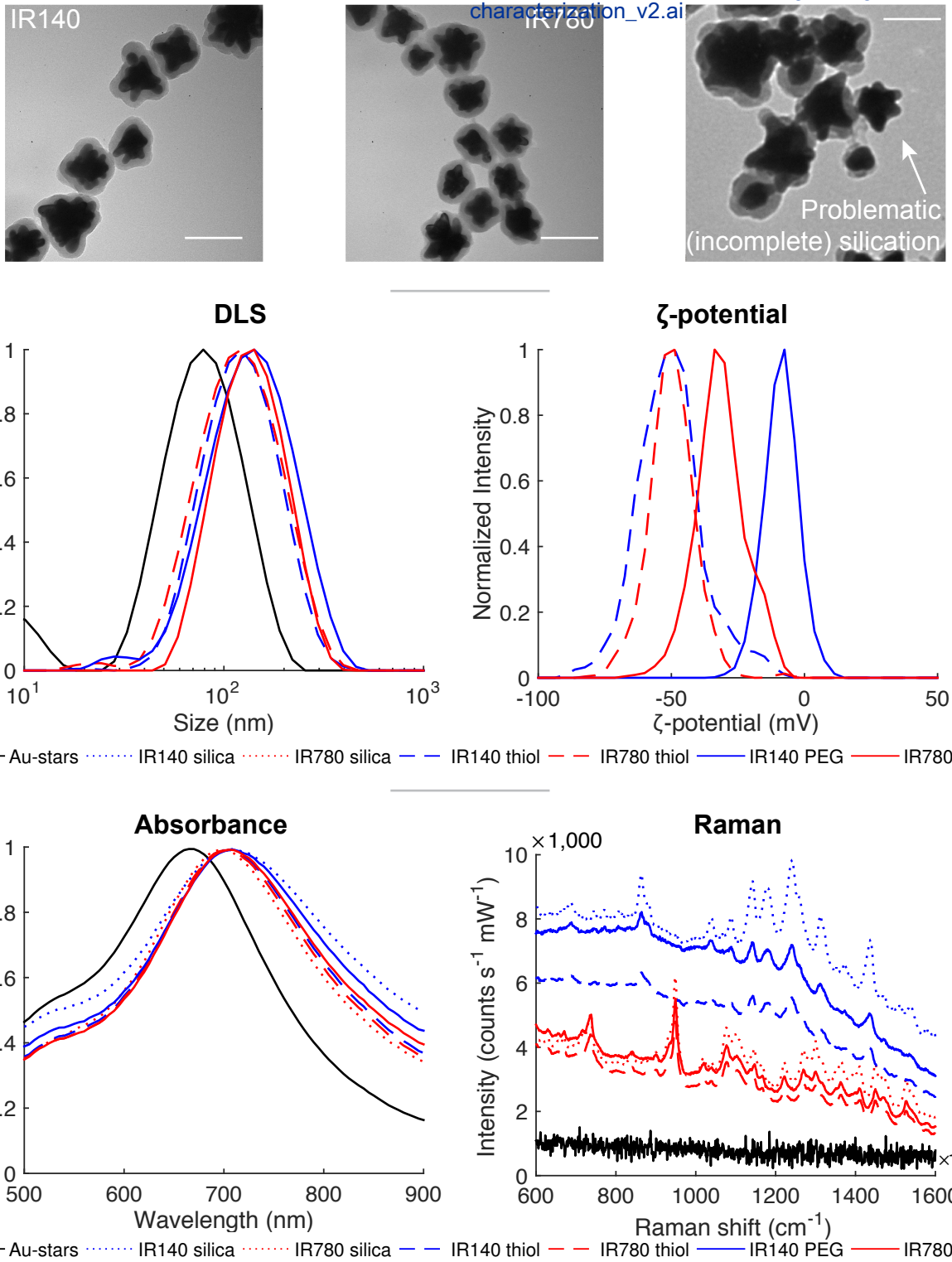

Figure 3

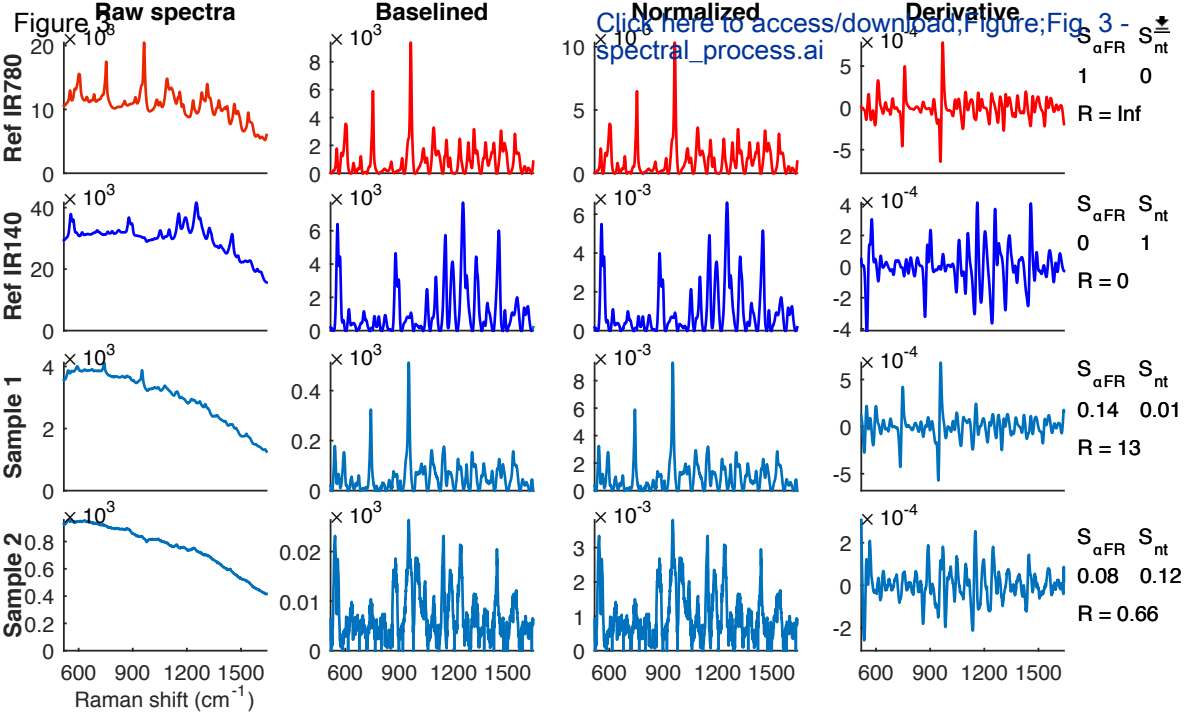

Figure 4

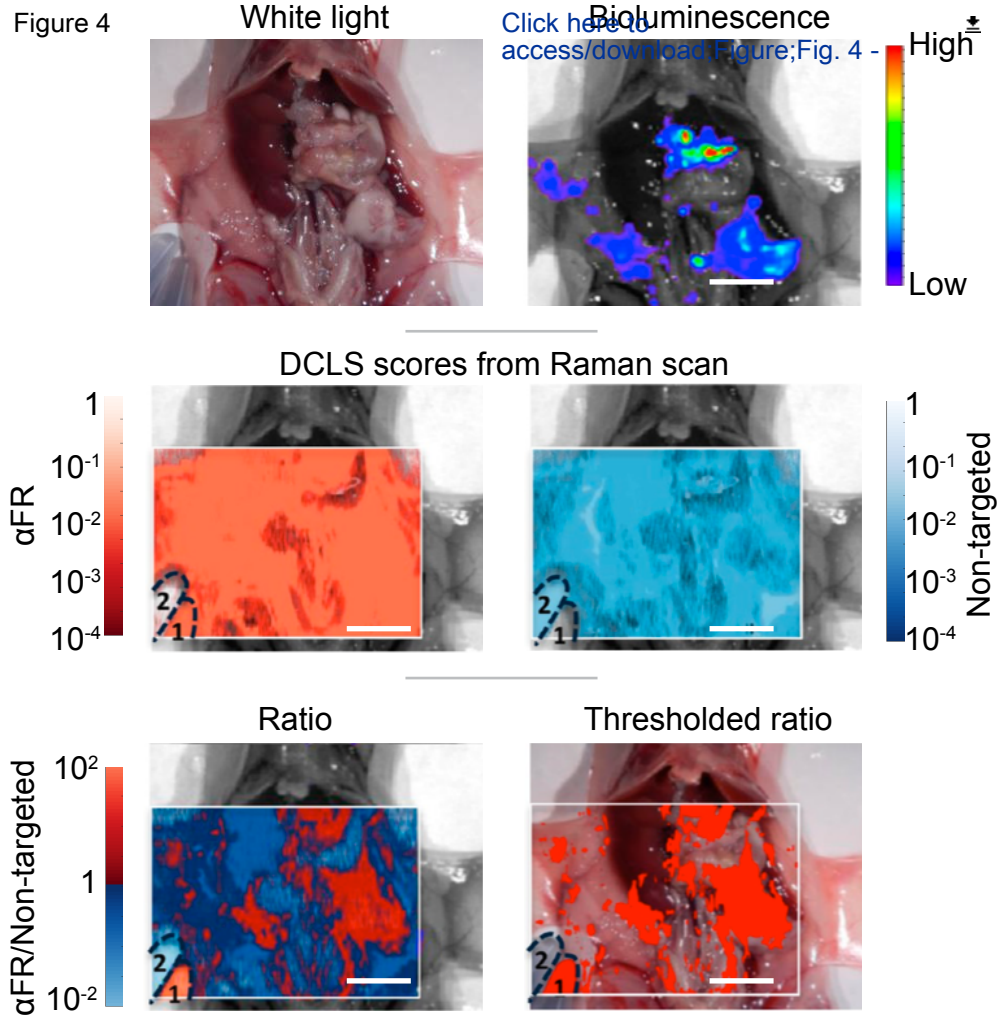

Step	Initial volume	Initial concentration	Final volume
1. Nanostar core	8 mL $HAuCl_4$	20 mM $HAuCl_4$	5 mL
2. Silication	1.2 mL	1.3 nM	1.2 mL
3.1. Thiolation	1 mL	0.5 nM	1 mL
3.5. Conjugation	1 mL	0.43 nM	1 mL

Table 1. Nanoparticle yield after each reaction step. The concentrations are approximate.

Final concentration
1.3 nM
0.5 nM
0.43 nM
0.39 nM

They were determined by nanoparticle tracking analysis, with two independent syntheses and 5 inc

lependent measurements from each.

Table of Materials

Click here to access/download;Table of Materials;JoVE_Materials.xlsx

Name of Reagent	Company	Catalog Number	Comments/Description
Ascorbic acid	Sigma-Aldrich	A5960	
3-MPTMS	Sigma-Aldrich	175617	
Ammonium hydroxide (28%)	Sigma-Aldrich	338818	
Anti-Folate Receptor antibody [LK26]	AbCam	ab3361	
Dimethyl sulfoxide	Sigma-Aldrich	276855	
Dimethyl sulfoxide (anhydrous)	Sigma-Aldrich	*276855*	
Ethanol	Sigma-Aldrich	792780	
IR140	Sigma-Aldrich	260932	
IR780 perchlorate*	Sigma-Aldrich	576409	Discontinued*
Isopropanol	Sigma-Aldrich	650447	
N.N.Dimethylformamide	Sigma-Aldrich	227056	
PEG crosslinker	Sigma-Aldrich	757853	
PEG-maleimide	Sigma-Aldrich	900339	
Tetrachloroauric Acid	Sigma-Aldrich	244597	
Tetraethyl Orthosilicate	Sigma-Aldrich	86578	
*IR792	Sigma-Aldrich	425982	*Alternative

Name of Equipment	Company	Catalog Number	Comments/Description
Dialysis cassette (3,500 MWCO)	ThermoFIsher	87724	
Centrifugal filters	Millipore	UFC510096	
inVia confocal Raman microscope	Renishaw		
MATLAB (v2014b)	Mathworks		
PLS Toolbox (v8.0)	Eigenvector research		

jove JOURNAL OF VISUALIZED EXPERIMENTS
1 Alewife Center #200
Cambridge, MA 02140
tel. 617.945.9051
www.jove.com

ARTICLE AND VIDEO LICENSE AGREEMENT

Title of Article: Surface-enhanced resonance Raman scattering nanoprobe ratiometry for the detection of microscopic ovarian cancer via folate receptor targeting

Author(s): Chrysafis Andreou, Anton Oseledchyk, Suchetan Pal, Moritz F. Kircher

Item 1 (check one box): The Author elects to have the Materials be made available (as described at http://www.jove.com/author) via: ☒ Standard Access ☐ Open Access

Item 2 (check one box):

☑ The Author is NOT a United States government employee.

☐ The Author is a United States government employee and the Materials were prepared in the course of his or her duties as a United States government employee.

☐ The Author is a United States government employee but the Materials were NOT prepared in the course of his or her duties as a United States government employee.

ARTICLE AND VIDEO LICENSE AGREEMENT

1. Defined Terms. As used in this Article and Video License Agreement, the following terms shall have the following meanings: "**Agreement**" means this Article and Video License Agreement; "**Article**" means the article specified on the last page of this Agreement, including any associated materials such as texts, figures, tables, artwork, abstracts, or summaries contained therein; "**Author**" means the author who is a signatory to this Agreement; "**Collective Work**" means a work, such as a periodical issue, anthology or encyclopedia, in which the Materials in their entirety in unmodified form, along with a number of other contributions, constituting separate and independent works in themselves, are assembled into a collective whole; "**CRC License**" means the Creative Commons Attribution-Non Commercial-No Derivs 3.0 Unported Agreement, the terms and conditions of which can be found at: http://creativecommons.org/licenses/by-nc-nd/3.0/legalcode; "**Derivative Work**" means a work based upon the Materials or upon the Materials and other pre-existing works, such as a translation, musical arrangement, dramatization, fictionalization, motion picture version, sound recording, art reproduction, abridgment, condensation, or any other form in which the Materials may be recast, transformed, or adapted; "**Institution**" means the institution, listed on the last page of this Agreement, by which the Author was employed at the time of the creation of the Materials; "**JoVE**" means MyJove Corporation, a Massachusetts corporation and the publisher of *The Journal of Visualized Experiments;* "**Materials**" means the Article and / or the Video; "**Parties**" means the Author and JoVE; "**Video**" means any video(s) made by the Author, alone or in conjunction with any other parties, or by JoVE or its affiliates or agents, individually or in collaboration with the Author or any other parties, incorporating all or any portion of the Article, and in which the Author may or may not appear.

2. Background. The Author, who is the author of the Article, in order to ensure the dissemination and protection of the Article, desires to have the JoVE publish the Article and create and transmit videos based on the Article. In furtherance of such goals, the Parties desire to memorialize in this Agreement the respective rights of each Party in and to the Article and the Video.

3. Grant of Rights in Article. In consideration of JoVE agreeing to publish the Article, the Author hereby grants to JoVE, subject to **Sections 4** and **7** below, the exclusive, royalty-free, perpetual (for the full term of copyright in the Article, including any extensions thereto) license (a) to publish, reproduce, distribute, display and store the Article in all forms, formats and media whether now known or hereafter developed (including without limitation in print, digital and electronic form) throughout the world, (b) to translate the Article into other languages, create adaptations, summaries or extracts of the Article or other Derivative Works (including, without limitation, the Video) or Collective Works based on all or any portion of the Article and exercise all of the rights set forth in (a) above in such translations, adaptations, summaries, extracts, Derivative Works or Collective Works and (c) to license others to do any or all of the above. The foregoing rights may be exercised in all media and formats, whether now known or hereafter devised, and include the right to make such modifications as are technically necessary to exercise the rights in other media and formats. If the "Open Access" box has been checked in **Item 1** above, JoVE and the Author hereby grant to the public all such rights in the Article as provided in, but subject to all limitations and requirements set forth in, the CRC License.

4. Retention of Rights in Article. Notwithstanding the exclusive license granted to JoVE in **Section 3** above, the Author shall, with respect to the Article, retain the non-exclusive right to use all or part of the Article for the non-commercial purpose of giving lectures, presentations or teaching classes, and to post a copy of the Article on the Institution's website or the Author's personal website, in each case provided that a link to the Article on the JoVE website is provided and notice of JoVE's copyright in the Article is included. All non-copyright intellectual property rights in and to the Article, such as patent rights, shall remain with the Author.

5. Grant of Rights in Video – Standard Access. This **Section 5** applies if the "Standard Access" box has been checked in **Item 1** above or if no box has been checked in **Item 1** above. In consideration of JoVE agreeing to produce, display or otherwise assist with the Video, the Author hereby acknowledges and agrees that, Subject to **Section 7** below, JoVE is and shall be the sole and exclusive owner of all rights of any nature, including, without limitation, all copyrights, in and to the Video. To the extent that, by law, the Author is deemed, now or at any time in the future, to have any rights of any nature in or to the Video, the Author hereby disclaims all such rights and transfers all such rights to JoVE.

6. Grant of Rights in Video – Open Access. This **Section 6** applies only if the "Open Access" box has been checked in **Item 1** above. In consideration of JoVE agreeing to produce, display or otherwise assist with the Video, the Author hereby grants to JoVE, subject to **Section 7** below, the exclusive, royalty-free, perpetual (for the full term of copyright in the Article, including any extensions thereto) license (a) to publish, reproduce, distribute, display and store the Video in all forms, formats and media whether now known or hereafter developed (including without limitation in print, digital and electronic form) throughout the world, (b) to translate the Video into other languages, create adaptations, summaries or extracts of the Video or other Derivative Works or Collective Works based on all or any portion of the Video and exercise all of the rights set forth in (a) above in such translations, adaptations, summaries, extracts, Derivative Works or Collective Works and (c) to license others to do any or all of the above. The foregoing rights may be exercised in all media and formats, whether now known or hereafter devised, and include the right to make such modifications as are technically necessary to exercise the rights in other media and formats. For any Video to which this Section 6 is applicable, JoVE and the Author hereby grant to the public all such rights in the Video as provided in, but subject to all limitations and requirements set forth in, the CRC License.

7. Government Employees. If the Author is a United States government employee and the Article was prepared in the course of his or her duties as a United States government employee, as indicated in **Item 2** above, and any of the licenses or grants granted by the Author hereunder exceed the scope of the 17 U.S.C. 403, then the rights granted hereunder shall be limited to the maximum rights permitted under such statute. In such case, all provisions contained herein that are not in conflict with such statute shall remain in full force and effect, and all provisions contained herein that do so conflict shall be deemed to be amended so as to provide to JoVE the maximum rights permissible within such statute.

8. Likeness, Privacy, Personality. The Author hereby grants JoVE the right to use the Author's name, voice, likeness, picture, photograph, image, biography and performance in any way, commercial or otherwise, in connection with the Materials and the sale, promotion and distribution thereof. The Author hereby waives any and all rights he or she may have, relating to his or her appearance in the Video or otherwise relating to the Materials, under all applicable privacy, likeness, personality or similar laws.

9. Author Warranties. The Author represents and warrants that the Article is original, that it has not been published, that the copyright interest is owned by the Author (or, if more than one author is listed at the beginning of this Agreement, by such authors collectively) and has not been assigned, licensed, or otherwise transferred to any other party. The Author represents and warrants that the author(s) listed at the top of this Agreement are the only authors of the Materials. If more than one author is listed at the top of this Agreement and if any such author has not entered into a separate Article and Video License Agreement with JoVE relating to the Materials, the Author represents and warrants that the Author has been authorized by each of the other such authors to execute this Agreement on his or her behalf and to bind him or her with respect to the terms of this Agreement as if each of them had been a party hereto as an Author. The Author warrants that the use, reproduction, distribution, public or private performance or display, and/or modification of all or any portion of the Materials does not and will not violate, infringe and/or misappropriate the patent, trademark, intellectual property or other rights of any third party. The Author represents and warrants that it has and will continue to comply with all government, institutional and other regulations, including, without limitation all institutional, laboratory, hospital, ethical, human and animal treatment, privacy, and all other rules, regulations, laws, procedures or guidelines, applicable to the Materials, and that all research involving human and animal subjects has been approved by the Author's relevant institutional review board.

10. JoVE Discretion. If the Author requests the assistance of JoVE in producing the Video in the Author's facility, the Author shall ensure that the presence of JoVE employees, agents or independent contractors is in accordance with the relevant regulations of the Author's institution. If more than one author is listed at the beginning of this Agreement, JoVE may, in its sole discretion, elect not take any action with respect to the Article until such time as it has received complete, executed Article and Video License Agreements from each such author. JoVE reserves the right, in its absolute and sole discretion and without giving any reason therefore, to accept or decline any work submitted to JoVE. JoVE and its employees, agents and independent contractors shall have

jove JOURNAL OF VISUALIZED EXPERIMENTS
1 Alewife Center #200
Cambridge, MA 02140
tel. 617.945.9051
www.jove.com

ARTICLE AND VIDEO LICENSE AGREEMENT

full, unfettered access to the facilities of the Author or of the Author's institution as necessary to make the Video, whether actually published or not. JoVE has sole discretion as to the method of making and publishing the Materials, including, without limitation, to all decisions regarding editing, lighting, filming, timing of publication, if any, length, quality, content and the like.

11. Indemnification. The Author agrees to indemnify JoVE and/or its successors and assigns from and against any and all claims, costs, and expenses, including attorney's fees, arising out of any breach of any warranty or other representations contained herein. The Author further agrees to indemnify and hold harmless JoVE from and against any and all claims, costs, and expenses, including attorney's fees, resulting from the breach by the Author of any representation or warranty contained herein or from allegations or instances of violation of intellectual property rights, damage to the Author's or the Author's institution's facilities, fraud, libel, defamation, research, equipment, experiments, property damage, personal injury, violations of institutional, laboratory, hospital, ethical, human and animal treatment, privacy or other rules, regulations, laws, procedures or guidelines, liabilities and other losses or damages related in any way to the submission of work to JoVE, making of videos by JoVE, or publication in *JoVE* or elsewhere by JoVE. The Author shall be responsible for, and shall hold JoVE harmless from, damages caused by lack of sterilization, lack of cleanliness or by contamination due to the making of a video by JoVE its employees, agents or independent contractors. All sterilization, cleanliness or decontamination procedures shall be solely the responsibility of the Author and shall be undertaken at the Author's expense. All indemnifications provided herein shall include JoVE's attorney's fees and costs related to said losses or damages. Such indemnification and holding harmless shall include such losses or damages incurred by, or in connection with, acts or omissions of JoVE, its employees, agents or independent contractors.

12. Fees. To cover the cost incurred for publication, JoVE must receive payment before production and publication the Materials. Payment is due in 21 days of invoice. Should the Materials not be published due to an editorial or production decision, these funds will be returned to the Author. Withdrawal by the Author of any submitted Materials after final peer review approval will result in a US$1,200 fee to cover pre-production expenses incurred by JoVE. If payment is not received by the completion of filming, production and publication of the Materials will be suspended until payment is received.

13. Transfer, Governing Law. This Agreement may be assigned by JoVE and shall inure to the benefits of any of JoVE's successors and assignees. This Agreement shall be governed and construed by the internal laws of the Commonwealth of Massachusetts without giving effect to any conflict of law provision thereunder. This Agreement may be executed in counterparts, each of which shall be deemed an original, but all of which together shall be deemed to me one and the same agreement. A signed copy of this Agreement delivered by facsimile, e-mail or other means of electronic transmission shall be deemed to have the same legal effect as delivery of an original signed copy of this Agreement.

A signed copy of this document must be sent with all new submissions. Only one Agreement required per submission.

CORRESPONDING AUTHOR:

Name:	Moritz F. Kircher
Department:	Radiology
Institution:	Memorial Sloan Kettering Cancer Center
Article Title:	Surface-enhanced resonance Raman scattering nanoprobe ratiometry for the detection of microscopic ovarian cancer via folate receptor targeting
Signature:	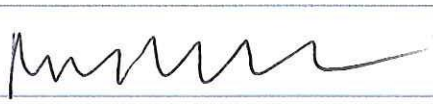 Date: 4/30/18

Please submit a signed and dated copy of this license by one of the following three methods:

1) Upload a scanned copy of the document as a pfd on the JoVE submission site;
2) Fax the document to +1.866.381.2236;
3) Mail the document to JoVE / Attn: JoVE Editorial / 1 Alewife Center #200 / Cambridge, MA 02139

For questions, please email submissions@jove.com or call +1.617.945.9051

JoVE submission JoVE58389 – Surface-enhanced resonance Raman scattering nanoprobe ratiometry for the detection of microscopic ovarian cancer via folate receptor targeting – Response to editorial and peer reviewer comments.

We would like to thank the editorial staff and the reviewers for their constructive comments. We have addressed the concerns and requirements to the best of our abilities, resulting to an improved manuscript.

Editorial comments:
Changes to be made by the Author(s):
1. Please take this opportunity to thoroughly proofread the manuscript to ensure that there are no spelling or grammar issues. The JoVE editor will not copy-edit your manuscript and any errors in the submitted revision may be present in the published version.
2. Please remove the embedded figure(s) and figure legends from the manuscript. Each figure must be accompanied by a title and a description after the Representative Results of the manuscript text.
3. Please remove the embedded Table from the manuscript. All tables should be uploaded separately to your Editorial Manager account in the form of an .xls or .xlsx file. Each table must be accompanied by a title and a description after the Representative Results of the manuscript text.
4. Figure 2: There are both “x 100” and “x 1,000” labels in the figure. Is “x 1,000” part of the y-axis scale label? Please clarify or move “x 1,000” to the left.
5. Please rephrase the Short Abstract to clearly describe the protocol and its applications in complete sentences between 10-50 words: “Here, we present a protocol to …”
6. Please rephrase the Abstract to more clearly state the goal of the protocol. A more detailed overview of the method and a summary of its advantages, limitations, and applications is appropriate. Please focus on the general types of results acquired.
7. Please rephrase the Introduction to include a clear statement of the overall goal of this method.
8. Please define all abbreviations before use.
9. Please use SI abbreviations for all units: L, mL, µL, h, min, s, etc.
10. Please remove all commercial language from your manuscript and use generic terms instead. All commercial products should be sufficiently referenced in the Table of Materials and Reagents.
For example: Amicon Ultra, CAS: 99126-64-4, Renishaw InVia, H&E, MATLAB (v2014b), PLS Toolbox (v8.0), etc.
11. Please move the ethics statement before your numbered protocol steps, indicating that the protocol follows the animal care guidelines of your institution.
12. 3.1: Please clarify when thiol is added and specify the amount of thiol added. How long is the ultrasonication done?
13. 5.3: Please specify all surgical instruments used. How large is the incision?
14. Lines 227-229: Please add these as a step or sub-step.
15. There is a 2.75 page limit for filmable content. Please highlight 2.75 pages or less of the Protocol (including headings and spacing) that identifies the essential steps of the protocol for the video, i.e., the steps that should be visualized to tell the most cohesive story of the Protocol. Remember that non-highlighted Protocol steps will remain in the manuscript, and therefore will still be available to the reader.
16. Please ensure that the highlighted steps form a cohesive narrative with a logical flow from one highlighted step to the next. Please highlight complete sentences (not parts of sentences). Please ensure that the highlighted part of the step includes at least one action that is written in imperative tense.
17. Please discuss any limitations of the technique.
18. References: Please do not abbreviate journal titles.
19. Please revise the table of the essential supplies, reagents, and equipment. The table should include the name, company, and catalog number of all relevant materials in separate columns in an xls/xlsx file.

Reviewers' comments:

Reviewer #1:
Minor Concerns:
The report is well written and the protocol is clearly explained. The results support the conclusion. I have comments related to the terminology used in the manuscript.
SERS and SERRS are well established techniques based on localized plasmon enhancement using metallic nanostructures. In the manuscript the authors use the terminology: SERS nanoparticles and 'surface enhanced resonance Raman scattering' (SERRS) nanoparticles. The addition of "nanoparticles" is unnecessary and confusing.
On page 3 you read: "molecularly targeted nanoparticle provides the specific signal, and a non-targeted control nanoparticle, with different Raman spectrum, accounts for non-specific background". Raman spectra are collected from molecules not nanoparticles.
The confusion persist when explaining the experiments: "Two distinct "flavors" of Raman nanoparticles are synthesized, each deriving its fingerprint from a different organic dye." In fact, the authors are using dye-embedded

core-shell nanoparticles for surface Raman enhancement (spectroscopic tags). For these special nanoparticles, the term "SERRS nanoprobe" (dye-embedded core-shell nanoparticles tailored for surface Raman enhancement) used later in the manuscript is adequate and avoid misunderstandings.

We thank the reviewer for pointing out this confusing terminology. We have edited the manuscript for more consistent use of the terms. We now use the term “nanoprobe” for the final construct (with antibody or PEG), and the term “nanoparticle” for the previous steps of synthesis (stars, silicated, and thiolated).

Reviewer #2:
In this manuscript, the authors provide a protocol to image ovarian cancer by SERS tags. The protocol includes: nanostar synthesis, silica formation, surface functionalization, mouse model, nanoparticle injection/imaging, data processing/visualization.
The protocol is definitely clear for the readers already working in the Rama tags field, especially for the tumor labelling. To broaden the readership, I suggest the authors add a figure to illustrate the "surface functionalization" because the readers in the related fields may be interested in the protocol but not familiar with those surface chemistry processes.
We have edited Figure 1 to include an extra step for the surface functionalization, and edited the caption accordingly.

In addition, I found that in this manuscript the recent related works cited (ref 21 to re 32) are all from the same journal (Nanotheranostics). Also, it is not critical but I would suggest authors also list other highly related works recently published in other journals.
We regret this oversight. We have added references from other journals.

Reviewer #3:
Manuscript Summary:
The authors propose to use SERRS spectroscopy on plasmonic core-shell particles targeting the most over-expressed membrane receptor in mouse ovarian cancer cells. The work is convincing and rather well written. Some aspects deserve to be clarified before publishing the work

Major Concerns:
- The introduction must be more informative about the possibility of discriminating between single cells in a tumor and not by SERS. A preliminary in vitro study would have helped to rationalize the level of non-specific interaction of the nanoprobe. Cite and discuss the following work in the introduction section:
Fasolato C, et al. Folate-based single cell screening using surface enhanced Raman microimaging. Nanoscale. 2016, 8, 17304.
We have added the related reference in the introduction.

- The authors report: "Typically, the size (hydrodynamic diameter) of the gold nanostar core is expected to be around 80 nm, and the silica shell is around 20 nm thick, making the total nanoparticle size around 120 nm" please explain.
The nanoparticle star-shaped gold core has a hydrodynamic diameter, as determined by DLS (Z-average) or nanoparticle tracking analysis, typically in the range of 80 nm. Once a spherical shell is formed around the core, approximately 20 nm in thickness (all around the core), the total diameter of the particle is 120 nm. This can be seen in the TEM images provided in Figure 2.

- Figure 3: The authors report the sentence "Absorbance maxima at lower wavelengths are a sign of either spherical morphology or aggregation." please explain. Why do you expect aggregation of nano-particles to cause a blue instead of a red shift?
As correctly pointed out by the reviewer, aggregation of spherical nanoparticles typically causes a bathochromic (“red”) shift of the plasmon resonance. Our particles have resonance in the red light region due to their star-shaped morphology. Aggregated nanostars give rise to less defined (more spherical) morphologies with plasmon resonance in the visible region, causing a hypsochromic (“blue”) shift.

- The author declare "After baseline subtraction, the fluorescence band is removed, the Raman peaks become prominent" florescence of what, please specify. Estimate the SERS gain factor by showing also the Raman dye control only.
As shown in the Figure 3, the raw spectra collected have a strong fluorescence band (the wide gaussian curve) on which the Raman bands are superimposed. The fluorescence mostly derives from the IR fluorescent dyes we used as Raman reporters. By using fluorescent dyes that absorb in the excitation wavelength, it is possible to achieve surface enhanced **resonance** Raman scattering, further enhancing the nanoprobe signal over other molecules that

do not absorb the excitation light. Although fluorescence in the vicinity of the gold nanoparticle is quenched for the most part, it is our understanding that residual dye molecules within the silica shell (several nm away from the gold) give rise to this fluorescent background. Unfortunately, the Raman signal of the free dye (without plasmonic enhancement) is negligible compared to the molecule's fluorescence, and we were not able to capture it without saturating our detector.

Specify with respect to what the spectra shown in figure 3 have been normalized. Specify in the methods the Raman calibration with respect to the grating used.
The spectra were normalized to have unit area (area under the curve = 1), as stated in the figure caption and also in Step 6.2. Calibration of the Raman scanner should be done according to the manufacturer's recommendation, and is typically performed using a common standard (e.g. a silicon wafer). We have added this recommendation to the text, in the discussion section.

Minor Concerns:
- in the final section of the work discuss whether such nanoprobe once targeted on the tumor might be employed also as a valuable therapeutic or theranostic tool.
We have added a paragraph discussing the theranostic potential of the probe in the discussion section.

Reviewer #4:
Manuscript Summary:
The manuscript describes a protocol for SERRS nanoparticle imaging for surgical tumor resection in small animal models. The protocol covers the chemistry behind fabrication and functionalization of the nanostar SERRS agents, their characterization in terms of successful manufacture. In addition, results are given for the use of the nano stars in an in vivo ovarian cancer small animal model. Ovarian cancer cells were injected in the peritoneum of immunocompromised mouse models, which constitutively express bioluminescent markers enabling their location to be tracked with optical imaging. The nano star model used was a so-called ratiometric model, in which nanoparticles of one color are non-targeted, and nanoparticles of another color are targeted for the folate receptor alpha. The idea is that the non-targeted nanoparticles will differentiate signal from successfully targeted nanoparticles, accounting for non-specific nanoparticle binding.

Major Concerns:
The primary concern with the protocol is that the method does not clearly demonstrate that the ratiometric targeting method actually works to identify residual micro metastases in the mouse model. The authors state that even targeted nanoparticles "tend to adhere onto the visceral surfaces even in the absence of their target." If this is true, then it is not clear how having additional nanoparticles which also have nonspecific binding will account for this limitation. In other words, why are 2 non-specific labels better than 1 non-specific label?
The targeted probe binds preferentially on the folate receptor, which is overexpressed by the tumor, but also sticks on other surfaces that are not cancerous. It is, therefore, incorrect to call it "nonspecific". However, when used on its own, it creates high background with many false-positive signals (Figure 4, middle left). The non-targeted probe coats the visceral surfaces in a similar way as the targeted-probe (Figure 4, middle right), but without increased accumulation in the areas of the folate receptor. By dividing the two signals, the non-specific adhesion is accounted for, and the increased accumulation in the areas of the overexpressed folate receptor is revealed.

The fact that the scheme may not work very well is demonstrated in Figure 4, where the location of tumor cells is indicated by the bioluminescence image, yet the thresholded ratio image does not seem to overlay the location of the bioluminescent (tumor) areas with any accuracy.
We regret that the reviewer feels that the accuracy is low. The perceived mismatch may be due differences between the two modalities (Raman vs bioluminescence imaging), the positioning of the animal related to the detector in each case, the dynamic range (sensitivity) of the detectors (10^2 for BLI, 10^4 for Raman), and focal plane of imaging. We would kindly refer to our related publication (doi:10.1021/acsnano.6b06796) where more extensive validation is performed.

In any case, no method to validate that the method actually works is provided. The method stops at simply describing how to display the image, but does not describe how the obtained images can be compared to ground truth (either from the bioluminescence imaging, or by sampling the cavity and doing pathology). This seems to be a major oversight or limitation of the protocol. If the authors could describe a method for validating the efficacy of the protocol, and also demonstrate that the protocol is efficacious, then it would be more suitable for publication in JOVE.
We believe we have validated our system sufficiently for our specific application, as described in our related publication. However, we would be delighted if more validation methods, more model systems, and more imaging scenarios were explored by other groups using our method. This is the reason we are providing the protocol, in a generalized format, so the community can validate it on their own systems, with new targets and other tumor types.

Minor Concerns:
There are some minor details that are missing or confusing. In Procedure 1.1 and 1.2, the gold solution is called different things (tetrachloroauric acid or gold trichloride). Whether the microscope used is upright or inverted is not specified, although the positioning of the animal in a supine position is prescribed.
We thank the reviewer for the observation, we have clarified these points in the text.